A Novel Anion-Binding Chiral Receptor Based on a Metalloporphyrin with Molecular Asymmetry. Highly Enantioselective Recognition of Amino Acid Derivatives

Katsuaki Konishi, Kazuyuki Yahara, Hiroshi Toshishige, Takuzo Aida, and Shohei Inoue*

Contribution from the Department of Synthetic Chemistry, Faculty of Engineering, University of Tokyo, Hongo, Bunkyo-ku, Tokyo 113, Japan

Received October 4, 1993®

Abstract: A chiral zinc strapped N-methylated porphyrin (**3c**) with molecular asymmetry, featuring a metal atom to bind a carboxylate anion and a rigid *p*-xylylene strap anchored via two amide linkages, was synthesized from mesoporphyrin II with enantiotopic faces, and the optical isomers of **3c** were resolved by HPLC. By using **3c** as a chiral receptor, the highly enantioselective binding was achieved for the carboxylate anions of *N*-benzyloxycarbonyl, *tert*-butoxycarbonyl, 3,5-dinitrobenzoyl, and acetyl amino acids. IR and NMR studies demonstrated the crucial role of the hydrogen bonding interaction between the receptor and substrates in the chiral recognition.

Introduction

The chemistry of chiral porphyrins is a subject of increasing interest in recent years in relation to developing new chiral auxiliaries and receptors for asymmetric synthesis and recognition[1,2] and providing potent tools for stereochemical understanding of the mechanisms of biologically important reactions.[3] Recently, we have succeeded in designing a series of chiral porphyrins by using as precursors porphyrins with C_{2h} or C_{4h} symmetry.[4] In the course of these studies, chiral strapped porphyrin complexes of manganese and iron were found to effectively catalyze asymmetric oxidation of prochiral olefins and sulfides, and satisfactorily high enantioselectivities were observed in the presence of a coordinating base such as imidazole.[5] In this case, imidazole coordinates to the catalyst from the unstrapped face so that the catalytic process occurs preferentially in the chiral strapped cavity with high steric requirements (Figure 1 (I)). This observation prompted us to design a novel chiral strapped *N*-alkylporphyrin complex (**3c**) whose unstrapped face is covalently blocked by the N-substituent (Figure 1 (II)). Within the strapped cavity of **3c**, the function-

Chart 1

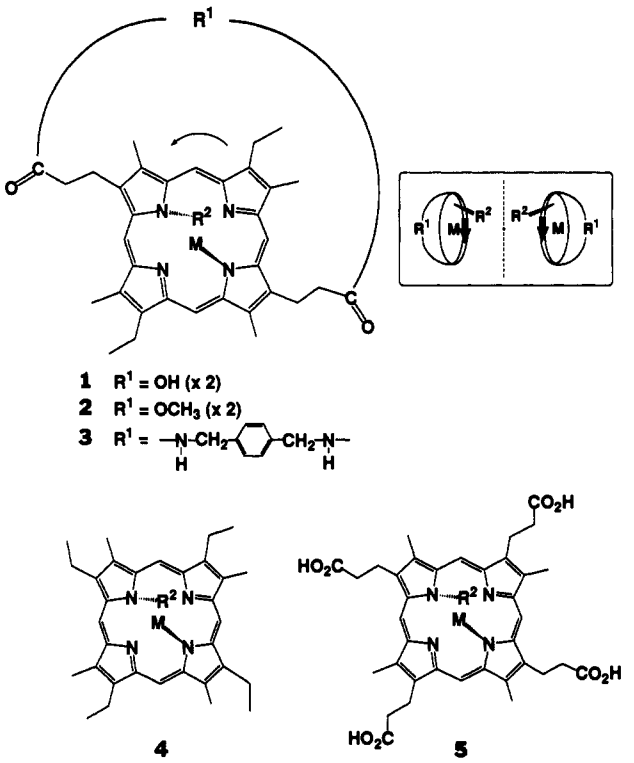

* Abstract published in *Advance ACS Abstracts,* February 1, 1994.

(1) For use of chiral porphyrins for asymmetric reactions, see: (a) Groves, J. T.; Myers, R. S. *J. Am. Chem. Soc.* **1983**, *105*, 5791. (b) Mansuy, D.; Battioni, P.; Renaud, J. P.; Guerin, P. *J. Chem. Soc., Chem. Commun.* **1985**, 155. (c) O'Malley, S.; Kodadek, T. J. *J. Am. Chem. Soc.* **1989**, *111*, 9116. (d) Groves, J. T.; Viski, P. *J. Am. Chem. Soc.* **1989**, *111*, 8537. (e) Groves, J. T.; Viski, P. *J. Org. Chem.* **1990**, *55*, 3628. (f) Naruta, Y.; Tani, F.; Maruyama, K. *Chem. Lett.* **1989**, 1269. (g) Naruta, Y.; Tani, F.; Maruyama, K. *J. Chem. Soc., Chem. Commun.* **1990**, 1378. (h) Naruta, Y.; Tani, F.; Ishihara, N.; Maruyama, K. *J. Am. Chem. Soc.* **1991**, *113*, 1378. (i) Naruta, Y.; Tani, F.; Maruyama, K. *Tetrahedron: Asymmetry:* **1991**, *2*, 533. (j) Naruta, Y.; Ishihara, N.; Tani, F.; Maruyama, K. *Chem. Lett.* **1991**, 1933. (k) Naruta, Y.; Tani, F.; Maruyama, K. *Tetrahedron Lett.* **1992**, *33*, 1269. (l) Collman, J. P.; Zhang, X.; Hembre, R. T.; Brauman, J. I. *J. Am. Chem. Soc.* **1990**, *112*, 5356. (m) Collman, J. P.; Zhang, X.; Lee, V. J.; Brauman, J. I. *J. Chem. Soc., Chem. Commun.* **1992**, 1647. (n) Halterman, R. L.; Jan, S.-T. *J. Org. Chem.* **1991**, *56*, 5253. (o) O'Malley, S.; Kodadek, T. *Tetrahedron Lett.* **1989**, *111*, 9116. (p) Maxwell, J. O.; O'Malley, S.; Brown, K.; Kodadek, T. *Organometallics* **1992**, *11*, 645. (q) O'Malley, S.; Kodadek, T. *Organometallics* **1992**, *11*, 2299. (r) Ohkubo, K.; Sagawa, T.; Kuwata, M.; Hata, T.; Ishida, H. *J. Chem. Soc., Chem. Commun.* **1989**, 352. (s) Ohkubo, K.; Sagawa, T.; Ishida, H. *Inorg. Chem.* **1992**, 2682.

(2) For use of chiral porphyrins for molecular recognition, see: (a) Le Maux, P.; Bahri, H.; Simonneaux, G. *J. Chem. Soc., Chem. Commun.* **1992**, 1350. (b) Aoyama, Y.; Uzawa, T.; Saita, K.; Tanaka, Y.; Toi, H.; Ogoshi, H. *Tetrahedron Lett.* **1988**, *29*, 5271. (c) Mizutani, T.; Ema, T.; Tomita, T.; Kuroda, Y.; Ogoshi, H. *J. Chem. Soc., Chem. Commun.* **1993**, 520. (d) Kuroda, Y.; Kato, Y.; Higashioji, T.; Ogoshi, H. *Angew. Chem., Int. Ed. Engl.* **1993**, *32*, 723.

(3) (a) Ortiz de Montellano, P. R.; Kunze, K. L.; Beilan, H. S. *J. Biol. Chem.* **1983**, *258*, 45. (b) Kunze, K. L.; Mangold, B. L. K.; Wheeler, C.; Beilan, H. S.; Ortiz de Montellano, P. R. *J. Biol. Chem.* **1983**, *258*, 4202. (c) Ortiz de Montellano, P. R.; Mangold, B. L. K.; Wheeler, C.; Kunze, K. L.; Reich, N. O. *J. Biol. Chem.* **1983**, *258*, 4208. (d) Augusto, O.; Kunze, K. L.; Ortiz de Montellano, P. R. *J. Biol. Chem.* **1982**, *257*, 6231. (e) Ortiz de Montellano, P. R.; Kunze, K. L. *Biochemistry* **1981**, *20*, 7266. (f) Swanson, B. A.; Ortiz de Montellano, P. R. *J. Am. Chem. Soc.* **1991**, *113*, 8146.

(4) (a) Kubo, H.; Aida, T.; Inoue, S.; Okamoto, Y. *J. Chem. Soc., Chem. Commun.* **1988**, 1015. (b) Konishi, K.; Miyazaki, K.; Aida, T.; Inoue, S. *J. Am. Chem. Soc.* **1990**, *112*, 5639. (c) Konishi, K.; Sugino, T.; Aida, T.; Inoue, S. *J. Am. Chem. Soc.* **1991**, *113*, 6487. (d) Konishi, K.; Takahata, Y.; Aida, T.; Inoue, S.; Kuroda, R. *J. Am. Chem. Soc.* **1993**, *115*, 1169.

(5) (a) Konishi, K.; Oda, K.; Nishida, K.; Aida, T.; Inoue, S. *J. Am. Chem. Soc.* **1992**, *114*, 1313. (b) Chiang, L.-c.; Konishi, K.; Aida, T.; Inoue, S. *J. Chem. Soc., Chem. Commun.* **1992**, 254.

0002-7863/94/1516-1337$04.50/0

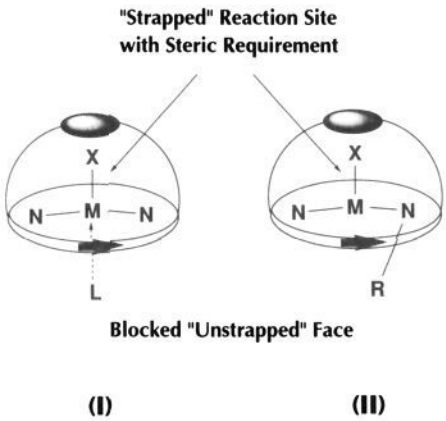

Figure 1. Chiral strapped metalloporphyrins. Schematic representations of the protection methods of the nonstrapped face for realizing enantioselective reaction: ligand coordination (I) and N-alkylation (II).

alities for (1) electrostatic (central metal), (2) hydrogen bonding (two amide linkages), and (3) van der Waals interactions are strategically incorporated.

In the present paper, we describe the synthesis, characterization, and utilization of this new chiral metalloporphyrin complex as a novel anion-binding chiral receptor. Design of enantioselective receptors has been a major objective in molecular recognition,[6] and asymmetric recognition of amino acids and derivatives has been most extensively studied. However, excellent enantioselections have been achieved only for amino acids in cationic (ammonium salt),[7] neutral (peptide[8] or amino acid ester[9]), and zwitterionic forms,[10] while the results are not satisfactory for amino acids in the form of carboxylate anions.[11] The present paper focuses attention on the enantioselective recognition of sodium salts of N-protected amino acids.

Results and Discussion

Synthesis and Characterization of Chiral Metalloporphyrin Receptor 3c. Synthesis of the racemate of **3c** was achieved in three steps from mesoporphyrin II (**1a**) having enantiotopic faces (Scheme 1). Condensation of the mixed acid anhydride of **1a** with 1,4-xylylenediamine gave *p*-xylylene-strapped porphyrin **3a** (Scheme 1 (i)),[5] which was reacted with methyl iodide to yield the strapped *N*-methylporphyrin **3b** (Scheme 1 (ii)).[12] The FAB-MS spectrum of **3b** showed a base peak at 681.3917 corresponding to MH^+. Since **3a** has two inequivalent pairs of the core nitrogen atoms, the N-methylated product (**3b**) should be a mixture of two possible regioisomers **3b-A,B** or either of them. In the ^1H and ^{13}C NMR spectra, **3b** showed single *N*-methyl signals at δ −4.46 and 32.3 ppm, respectively. When the strap moiety of **3b** was removed by acidolysis of the amide linkages followed by esterification (Scheme 1 (iii)), the zinc acetate complex of the resulting *N*-methylmesoporphyrin II dimethyl ester (**2c**) again exhibited single ^1H (δ −4.71) and ^{13}C (δ 35.4) signals due to the *N*-methyl group. In contrast, direct N-methylation of mesoporphyrin II dimethyl ester (**2a**) followed by metalation with $Zn(OAc)_2$ afforded a regioisomeric mixture of **2c-A,B** (Scheme 1 (iv)), which showed two well-distinguishable *N*-methyl signals at δ −4.67 and −4.71 ppm (intensity ratio = 52:48) in the ^1H NMR spectrum and the corresponding ^{13}C NMR signals at δ 34.0 and 35.5 ppm. Thus, **3b** is not a regioisomeric mixture but either of the regioisomers **3b-A,B**. In order to specify the position of the alkylated nitrogen atom in **3b**, the zinc acetate complexes of *N*-methyletioporphyrin I (**4c**) and *N*-methylcoproporphyrin I tetramethyl ester (**5c**) were prepared as reference complexes, which showed the *N*-methyl signals respectively at δ 34.0 and 35.6 ppm in the ^{13}C NMR spectra. By comparison of the chemical shift values of these characteristic signals with the *N*-methyl signal of **2c**, **3b** was identified as the isomer **3b-A** with the methyl group attached to the nitrogen atom of a strapped pyrrole ring.

Treatment of **3b-A** thus obtained with methanolic $Zn(OAc)_2$ yielded the zinc complex **3c** quantitatively (Scheme 1 (v)), which exhibited a FAB-MS molecular peak (M^+) at m/z 802 and a peak corresponding to $[M - OAc]^+$ at m/z 743.3052. The ^1H NMR spectrum of **3c** showed four β-methyl signals at δ 3.73, 3.68, 3.51, and 3.16, where the most upfield signal (δ 3.16) is assignable to the β-methyl group (H^3) in the N-methylated pyrrole ring (Figure 2), taking into account the general trends in the ^1H NMR profiles of *N*-alkylporphyrins.[13] With the aid of double-quantum-filtered COSY (DQF-COSY) and NOESY measurements, all the protons in **3c** were unambiguously assigned (Table 1). The protons of the peripheral β-methyl groups (H^3, H^8, H^{13}, and H^{18}) and methylene units attached to the pyrrole β positions (H^{7A}, H^{17A}, H^a, $H^{a'}$, H^j, and $H^{j'}$) and meso positions (H^α, H^β, H^γ, and H^δ) were vicinally related to each other in the NOESY spectrum, where the cross peaks were observed for the pairs $H^{b'}/H^c$ (or H^d),[14] $H^{i'}/H^h$ (or H^g),[14] H^e/H^d, $H^e/H^{d'}$, H^f/H^g, and $H^f/H^{g'}$. In the ^1H NMR spectrum of **3c**, the *N*-methyl signal was observed at δ −4.05, which is downfield from that of the unstrapped complex **4c** (δ −4.68), indicating a possible distortion of the porphyrin skeleton of **3c** induced by strapping.[15] Despite this weakened shielding effect of the porphyrin ring, the axial acetate signal of **3c** was observed at a higher field (δ −1.32) than that of **4c** (δ −1.04). A more remarkable difference was observed for the zinc *N*-Cbz-glycinate complexes **3d** and **4d**, where the signals due to the ZnO_2CCH_2 (δ −2.21) and *N*-methyl (δ −3.87) moieties in the strapped complex (**3d**) were respectively 2.69 ppm upfield and 0.71 ppm downfield from those of the unstrapped complex (**4d**) (ZnO_2CCH_2, δ 0.48; *N*-methyl, δ −4.58). These observations strongly indicate that the zinc strapped *N*-methylporphyrins have the structure shown in Figure 2, where the *N*-methyl group is located on the unstrapped face, while the axial

(6) For recent examples, see: (a) Tsukube, H.; Sohmiya, H. *J. Org. Chem.* **1991**, *56*, 875. (b) Lindoy, L. F.; Walker, G. W.; Everett, G. W. *J. Am. Chem. Soc.* **1990**, *112*, 3659. (c) Castro, P. P.; Georgiadis, T. M.; Diederich, F. *J. Org. Chem.* **1989**, *54*, 5834. (d) Pirkle, W. H.; Doherty, E. M. *J. Am. Chem. Soc.* **1989**, *111*, 4113. (e) Petti, M. A.; Shepodd, T. J.; Barrans, R. E., Jr.; Dougherty, D. A. *J. Am. Chem. Soc.* **1988**, *110*, 6825. (f) Pirkle, W. H.; Pochapsky, T. C. *J. Am. Chem. Soc.* **1987**, *109*, 5975. (g) Pirkle, W. H.; Reno, D. S. *J. Am. Chem. Soc.* **1987**, *109*, 7189.

(7) (a) Peacock, S. C.; Domeier, L. A.; Gaeta, F. C. A.; Helgeston, R. C.; Timko, J. M.; Cram, D. J. *J. Am. Chem. Soc.* **1978**, *100*, 8190 and references cited therein. (b) Davidson, R. B.; Bradshaw, J. S.; Jones, B. A.; Dalley, N. K.; Christensen, J. J.; Izatt, R. M. *J. Org. Chem.* **1984**, *49*, 353. (c) Maruyama, K.; Sohmiya, H.; Tsukube, H. *J. Chem. Soc., Chem. Commun.* **1989**, 864. (d) Naemura, K.; Fukunaga, R.; Yamanaka, M. *J. Chem. Soc., Chem. Commun.* **1985**, 1560.

(8) (a) Sanderson, P. E. J.; Kilburn, J. D.; Still, W. C. *J. Am. Chem. Soc.* **1989**, *111*, 8314. (b) Sanderson, P. E. J.; Still, W. C. *J. Org. Chem.* **1990**, *55*, 5184. (c) Jeong, K.-S.; Muehldorf, A. V.; Rebek, J., Jr. *J. Am. Chem. Soc.* **1990**, *112*, 6144. (d) Hong, J.-I.; Namgoong, S. K.; Bernardi, A.; Still, W. C. *J. Am. Chem. Soc.* **1991**, *113*, 5111. (e) Yoon, S. S.; Still, W. C. *J. Am. Chem. Soc.* **1993**, *115*, 823.

(9) (a) Rebek, J., Jr.; Askew, B.; Ballester, P.; Doa, M. *J. Am. Chem. Soc.* **1987**, *109*, 4119. (b) References 2c,d.

(10) (a) Lipkowitz, K. B.; Raghothama, S.; Yang, J.-I. *J. Am. Chem. Soc.* **1992**, *114*, 1554. (b) Galan, A.; Andreu, D.; Echavarren, A. M.; Prados, P.; de Mendoza, J. *J. Am. Chem. Soc.* **1992**, *114*, 1511.

(11) Echavarren, A.; Galan, A.; Lehn, J. M.; de Mendoza, J. *J. Am. Chem. Soc.* **1989**, *111*, 4994.

(12) Cavaleiro, J. A. S.; Condesso, M. F. P. N.; Jackson, A. H.; Neves, M. G. P. M. S.; Rao, K. R. N.; Sadashiva, B. K. *Tetrahedron Lett.* **1984**, *25*, 6047.

(13) (a) Jackson, A. H.; Dearden, G. R. *Ann. N. Y. Acad. Sci.* **1973**, *206*, 151. (b) Kunze, K. L.; Ortiz de Montellano, P. R. *J. Am. Chem. Soc.* **1981**, *103*, 4225.

(14) The signals of H^e and H^h were overlapped with those of H^d and H^g, respectively.

(15) The intensity ratio of Q-band III (535 nm) to Q-band IV (501 nm) of **3a** (0.88) was higher than that of the unstrapped analogue **2a** (0.73). A similar tendency has been reported for some distorted strapped porphyrins: Morgan, B.; Dolphin, D.; Jones, R. H.; Jones, T.; Einstein, F. W. B. *J. Org. Chem.* **1987**, *52*, 4628.

Scheme 1

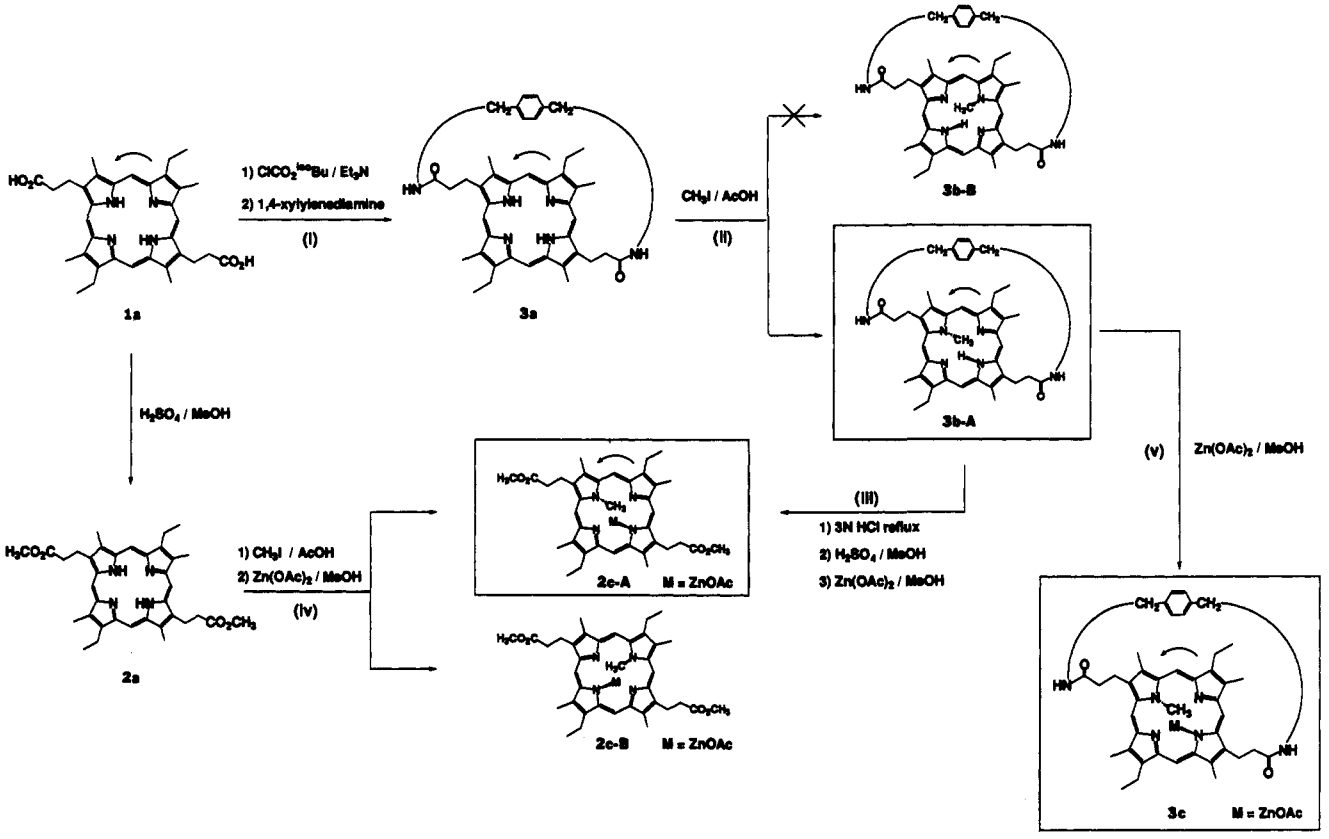

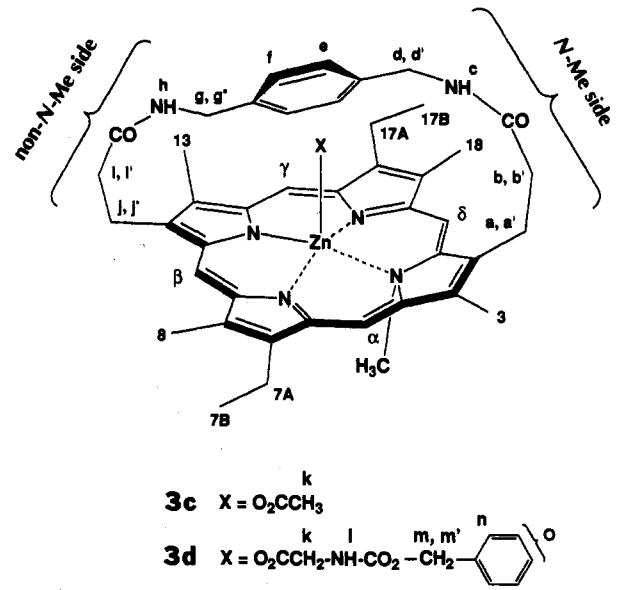

Figure 2. Schematic representations of one enantiomer of the zinc acetate complex of the strapped *N*-methylporphyrin **3c** and that of the zinc *N*-Cbz-glycinate complex **3d**.

group is on the strapped face and receives a shielding effect by the proximate *p*-xylylene unit.[16]

CPK model studies on **3c** indicate that the cavity of the strap is too small for the axial ligand to flip from one side of the strap to the other, and therefore two structural isomers **3c-A,B** (Figure 3) are anticipated for **3c**. When the molecular structure of **3c** is divided by the strap into two parts, the isomer **3c-A** has the axial acetate group on the opposite side of the strap from the *N*-methyl group, while in the isomer **3c-B**, these two groups are located on the same side. Considering the single *N*-methyl signal and the four signals, respectively, for the meso and β-methyl protons (Table 1), **3c** is not a mixture of **3c-A,B** but a single isomer with four inequivalent pyrrole units. In this connection, a NOESY cross peak was observed between the H^{13} protons and the phenylene protons (H^f) (Figure 2). Since such a contact is unlikely for the isomer **3c-A** from the CPK model, the isomer **3c-B** is the plausible candidate.

The ^1H NMR profile as to the strap moiety of **3c-B** indicates the lack of symmetry in this molecule. For instance, the signals due to the two amide NH moieties are 0.9 ppm apart (Table 1), where one (H^c) in the strap linked to the N-methylated pyrrole ring (denoted as "*N*-Me side") is observed at δ 3.47, while the other (H^h) on the opposite, "non-*N*-Me side" is observed at a lower field (δ 4.34). Similarly, the other protons on the "*N*-Me side", (H^b, $H^{b'}$, H^d, $H^{d'}$, and H^e) are more shielded than the corresponding protons on the "non-*N*-Me side" (H^i, $H^{i'}$, H^g, $H^{g'}$, and H^f). Thus, the strap cavity in **3c-B** is of a distorted shape, where the two amide functionalities are topologically inequivalent from the central metal.

Optical Resolution of the Zinc Complex of Strapped *N*-Methylporphyrin 3c. The antipodes of the zinc acetate complex **3c** were resolved in optically pure forms by chiral HPLC (Daicel, CHIRALCEL OD)[4,5] with hexane/2-propanol/acetic acid (90/9/1 v/v) as the eluent (Figure 4). The compounds corresponding to these two peaks (fractions I and II) showed perfect mirror-image circular dichroism (CD) spectra of each other (Figure 5, (i) and (ii)), where a split Cotton effect was observed in the Soret region. Fraction I (fraction II) showed a positive (negative) CD band at 422 nm with [Θ] of 172 000 (−172 000) deg·cm²·dmol⁻¹ and a negative (positive) one at 436 nm with [Θ] of −169 000 (160 000) deg·cm²·dmol⁻¹. Thus, in the following part, the antipodes corresponding to fractions I and II are denoted for convenience as $[+]_{422}$- and $[-]_{422}$-**3c**, respectively. In contrast

(16) There has been reported no crystallographically defined N-substituted porphyrin complex with the axial ligand and N-substituent on the same face of the porphyrin moiety: Lavallee, D. K. *The Chemistry and Biochemistry of N-Substituted Porphyrins*; VCH: New York, 1987; pp 7–39 and references cited therein.

Table 1. ^{1}H NMR Chemical Shifts (δ, ppm) and Coupling Constants (Hz, in Parentheses) for **3c**,**d**[a]

atom[b]	3c		3d	
meso				
α	9.98	s	10.02	s
β	9.92	s	9.96	s
γ	10.24	s	10.29	s
δ	10.12	s	10.32	s
β-methyl				
3	3.16	s	3.08	s
8	3.52	s	3.55	s
13	3.68	s	3.78	s
18	3.73	s	3.78	s
β-ethyl				
7A	4.17	q (7.6)	4.18	q (7.5)
7B	2.00	t (7.6)	1.97	t (7.5)
17A	4.00	q (7.8)	4.00	q (7.6)
17B	1.80	t (7.8)	1.75	t (7.6)
strap				
a	4.35	m	4.45	m
a′	3.90	m	3.96	m
b	2.45	dd (10.2, 12.2)	2.32	dd (10.5, 12.3)
b′	0.70	dd (12.2, 12.2)	1.12	dd (12.3, 12.3)
c	3.47	s	4.54	s, br
d	3.46	d (12.2)	3.12	d (12.4)
d′	2.07	d (12.2)	1.69	d (12.4)
e	4.67	d, br (7.9)	4.30	s, br
f	5.36	d, br (7.9)	5.06	d, br (8.0)
g	4.43	d (12.2)	4.35	d (12.3)
g′	2.71	d (12.2)	2.11	d (12.3)
h	4.34	s, br	6.05	s, br
i	3.04	ddd (12.5, 4.3, 12.2)	3.20	m
i′	2.76	ddd (12.5, 4.8, 2.5)	2.94	m
j	4.47	m	4.48	m
j′	4.35	m	4.48	m
N-CH_3	−4.05	s	−3.87	s
axial ligand				
k	−1.32	s	−2.33	m
l			3.46	s
m			4.60	d (13.0)
m′			4.76	d (13.0)
n			7.03	m
o			7.18	m

[a] In $CDCl_3$ (0.02 M) at 30 °C. Assignments were made with the aid of 2D ^{1}H–^{1}H DQF-COSY and NOESY NMR spectroscopies. [b] Atom labeling is shown in Figure 2.

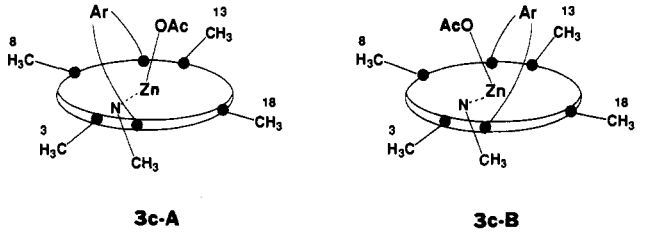

3c-A **3c-B**

Figure 3. Schematic representations of two possible structural isomers of **3c**.

with the zinc complex, the antipodes of the free base strapped N-methylporphyrin **3b**, derived from $[+]_{422}$- and $[-]_{422}$-**3c**, showed much smaller CD bands at the Soret region (412 nm) ($|[\Theta]|_{max}$ = 25 000 deg·cm^2·dmol^{-1} at 378 nm) (Figure 5 (iii and iv)). With respect to the absolute configuration at the methylated nitrogen atom in **3c**, **2c** derived from $[+]_{422}$-**3c** showed a negative CD band ($|[\Theta]|_{max}$ = 20 000 deg·cm^2·dmol^{-1} at 436 nm), which is similar to the CD profile observed for the zinc complex of (*S*)-*N*-(2-hydroxyethyl)etioporphyrin I.[17]

Chiral Recognition of Amino Acid Derivatives. Zinc complexes of N-substituted porphyrins are known to undergo axial ligand exchange with various anions. Thus, asymmetric binding of the

(17) Reference 4d.

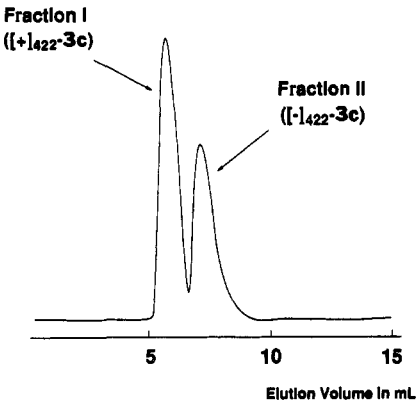

Figure 4. HPLC profile of **3c** using the analytical column (see the Experimental Section) with hexane/2-propanol/acetic acid (90/9/1 v/v) as the eluent at room temperature, monitored at 430 nm.

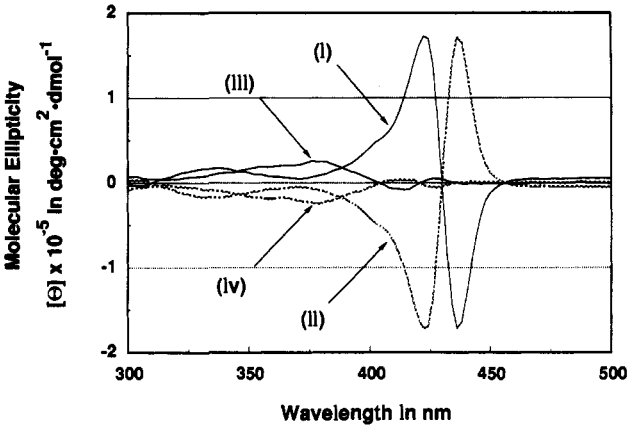

Figure 5. CD spectra of the antipodes of **3c** ($[+]_{422}$-**3c** (i) and $[-]_{422}$-**3c** (ii) corresponding to fractions I and II in Figure 4, respectively) in $CHCl_3$ (4.0×10^{-5} M) and those of **3b** ($[+]_{378}$-**3b** (iii) and $[-]_{378}$-**3b** (iv) derived from $[+]_{422}$-**3c** and $[-]_{422}$-**3c**, respectively) in $CHCl_3$/triethylamine (90/10 v/v) (3.5×10^{-5} M) at room temperature.

carboxylate anions of amino acids to **3c** was investigated. Within the binding site of **3c** are arranged (i) a metal atom (Zn) to bind a carboxylate anion, (ii) two chemically inequivalent amide functionalities with hydrogen bonding capability, and (iii) a rigid strap as a wall for van der Waals interactions with substrates.

The asymmetric binding with **3c** was carried out by single extraction of sodium salts of N-protected amino acids in $CHCl_3$/water. For example, when a $CHCl_3$ solution of $[+]_{422}$-**3c** was shaken for 15 s with an aqueous solution of *N*-(benzyloxycarbonyl)-DL-valine (*N*-Cbz-DL-Val) sodium salt (2 equiv), axial ligand exchange took place smoothly and quantitatively to give a mixture of two diastereoisomeric zinc *N*-Cbz-valinate complexes, L-$[+]_{422}$-**3e** and D-$[+]_{422}$-**3e** (X = $O_2CC^*H(i\text{-}Pr)NHCbz$) (Scheme 2),[18] which were identified on the basis of ^{1}H NMR spectra of the authentic samples prepared from $[+]_{422}$-**3c** with D- and L-*N*-Cbz-valine sodium salts. The mole ratio of the two diastereoisomers ([L-$[+]_{422}$-**3e**]:[D-$[+]_{422}$-**3e**]) was 92:8, as determined by the relative intensity of the diastereoisomerically split *N*-methyl signals (δ −4.13 for L-$[+]_{422}$-**3e** and δ −4.03 for D-$[+]_{422}$-**3e** (X = $O_2CC^*H(i\text{-}Pr)NHCbz$)). Upon treatment of the above mixture with trifluoroacetic acid, the complexes were completely demetalated to release *N*-Cbz-valine with an L:D ratio, as determined by HPLC, of 90:10. Thus, the $[+]_{422}$-receptor preferentially binds the L-isomer of *N*-Cbz-valinate.

Table 2 summarizes results of the single extraction of a variety of racemic substrates with racemic **3c** (Scheme 3), where the high enantioselectivities with the ratios of the major to the minor

(18) L-$[+]_{422}$-**3e** and D-$[+]_{422}$-**3e** showed virtually identical CD profiles to that of $[+]_{422}$-**3c**.

Scheme 2

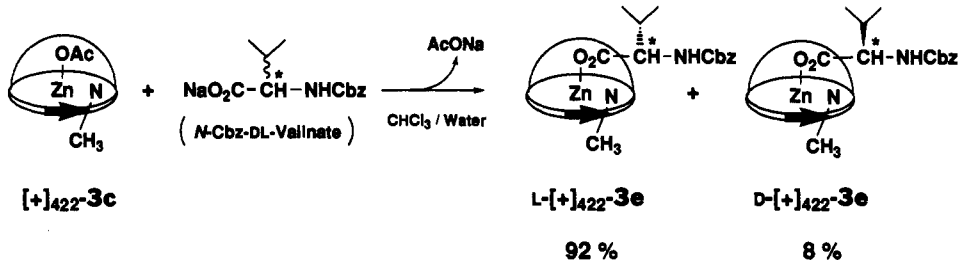

Scheme 3

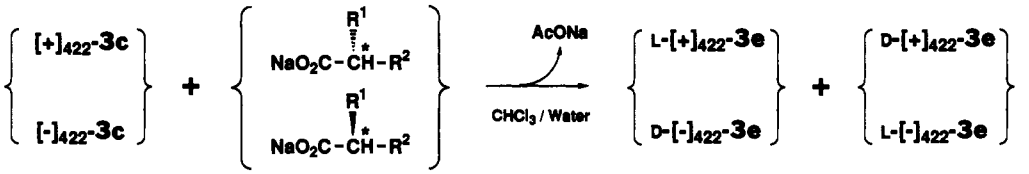

Table 2. Single Extraction of the Sodium Salts of Racemic N-Protected Amino Acids with Racemic 3c

run	substrate[a]	[L-[+]$_{422}$- + D-[−]$_{422}$-3e]/[L-[−]$_{422}$- + D-[+]$_{422}$-3e]
1	*N*-Cbz-alaninate	91/9 (10.1)
2	*N*-Cbz-*N*-methylalaninate	50/50 (1.0)
3	*N*-Cbz-valinate	96/4 (21.2)
4	*N*-Boc-valinate	95/5 (19.9)
5	*N*-acetylvalinate	85/15 (5.6)
6	*N*-Cbz-norvalinate	91/9 (9.9)
7	*N*-Cbz-leucinate	85/15 (5.8)
8	*N*-Cbz-norleucinate	88/12 (7.4)
9	*N*-Cbz-prolinate	50/50 (1.0)
10	*N*-Cbz-methioninate	91/9 (10.2)
11	*N*-Cbz-serinate	23/77 (0.3)
12	*N*-Cbz-phenylglycinate	91/9 (9.6)
13	*N*-(3,5-dinitrobenzoyl)phenylglycinate	96/4 (23.4)
14	*N*-Cbz-phenylalaninate	84/16 (5.1)
15	*N*-Cbz-tryptophanate	89/11 (8.5)

[a] Cbz = benzyloxycarbonyl; Boc = *tert*-butoxycarbonyl.

diastereoisomer pairs of 96:4 to 84:16 were observed for the substrates having NHCO moieties (runs 1, 3-8, and 10-15). Except for the case of *N*-Cbz-serinate having a hydroxyl functionality with hydrogen bonding capability (run 11), [+]$_{422}$- and [−]$_{422}$-receptors preferentially bind L- and D-substrates, respectively. Among the substrates examined, the highest enantioselectivity was observed for *N*-(3,5-dinitrobenzoyl)phenylglycinate, where the ratio [L-[+]$_{422}$- + D-[−]$_{422}$-3e]/[L-[−]$_{422}$- + D-[+]$_{422}$-3e] of 23.4 was achieved (run 13). As for the effect of the N-protecting group of the substrate, the enantioselectivity for *N*-(*tert*-butoxycarbonyl)valinate (19.9, run 4) was comparably higher than that for the *N*-Cbz analogue (21.2, run 3), while the *N*-acetyl analogue was less enantioselectively recognized (5.8, run 5). In sharp contrast, no enantioselection took place for *N*-Cbz-*N*-methylalaninate and *N*-Cbz-prolinate having no NHCO functionalities (runs 2 and 9).

Mechanism of Chiral Recognition. The high degree of chiral recognition achieved here is considered a result of multiple interactions between the chiral receptor and the substrates. Evidence for hydrogen bond formation between the NHCO moieties of the receptor and the substrates was provided by IR and ^{1}H NMR studies coupled with two-dimensional DQF-COSY and NOESY measurements. The zinc acetate complex **3c** showed a single amide C=O stretching infrared absorption at 1645 cm^{-1} in $CHCl_3$ (Figure 6 (i)), while the *N*-Cbz-glycinate complex **3d** showed an additional amide C=O absorption at a lower wavenumber (1622 cm^{-1}) with a comparable intensity to that at 1645 cm^{-1} (Figure 6 (ii)). This observation indicates the participation of either of the two amide C=O groups at the strap moiety of the receptor in hydrogen bonding interaction with the

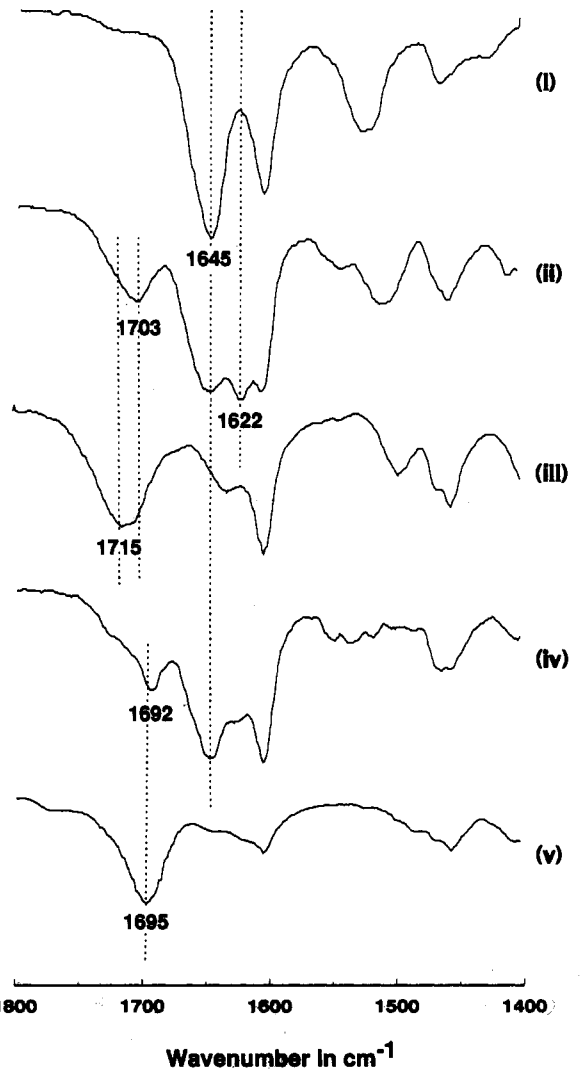

Figure 6. IR spectra of the zinc carboxylate complexes in $CHCl_3$ (5×10^{-3} M) at 25 °C: zinc acetate complex **3c** (i) and zinc *N*-Cbz-glycinate complex **3d** (ii) of the strapped *N*-methylporphyrin, zinc *N*-Cbz-glycinate complex of *N*-methyletioporphyrin I (**4d** (iii)), zinc *N*-methyl-*N*-Cbz-glycinate complex of the strapped *N*-methylporphyrin **3d'** (iv), and zinc *N*-methyl-*N*-Cbz-glycinate complex of *N*-methyletioporphyrin I (**4d'** (v)).

binding substrate. As for the carbamate C=O group in the substrate, the *N*-Cbz-glycinate in **3d** showed the C=O stretching absorption at 1703 cm^{-1} (Figure 6 (ii)), which is lower in wavenumber than that for the unstrapped reference complex (**4d**,

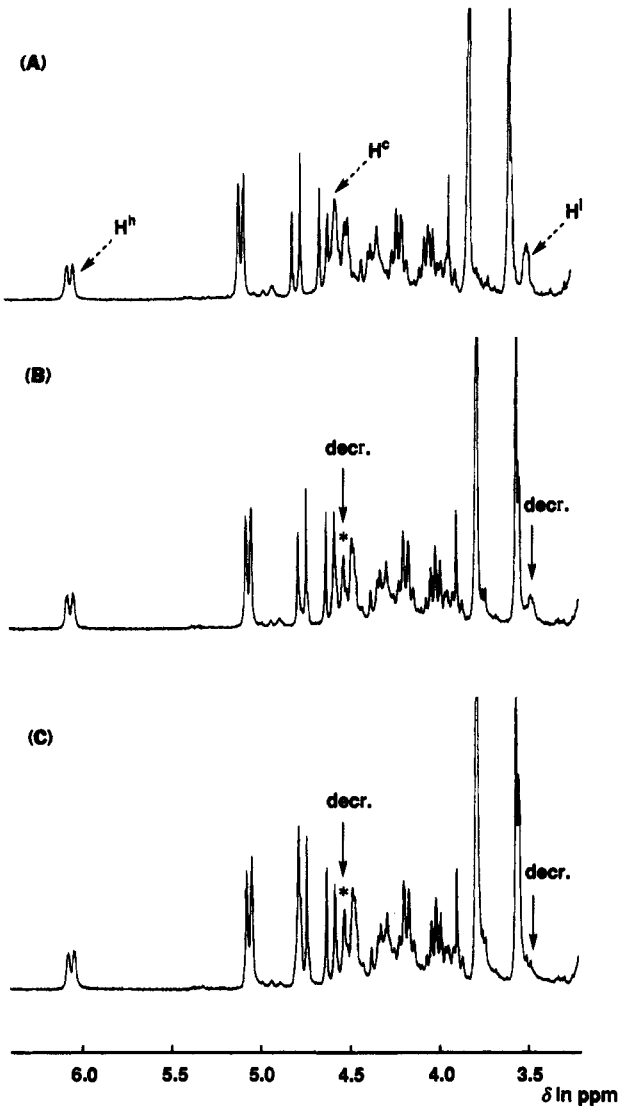

Figure 7. ^{1}H NMR spectra of the zinc *N*-Cbz-glycinate complex **3d** in $CDCl_3$ (5×10^{-2} M) at 25 °C (A) and after stirred with D_2O for 0.5 h (B) and 3 h (C). Asterisks indicate the signals due to the protons H^j, $H^{j'}$, H^a, and H^m.

1715 cm^{-1} (Figure 6 (iii))). Thus, upon binding of *N*-Cbz-glycinate with the receptor, two different hydrogen bonding interactions operate, where one of the strap amide C=O groups in the receptor and the carbamate C=O group in the binding substrate are involved.

Since hydrogen-bonded NH groups are known to be reluctant to undergo deuterium exchange,[19] the three different NH groups in **3d** are expected to show different exchange activities. When a $CDCl_3$ solution of **3d** (0.05 mmol, 1 mL) (Figure 7A) was vigorously stirred with D_2O (1 mL) for 0.5 h at room temperature, the signal due to the amide proton H^c (δ 4.54) on the "*N*-Me side" of the strap (Figure 2) disappeared completely, while that on the "non-*N*-Me side" (H^h, δ 6.05) remained without any decrease in intensity (Figure 7B), even after being stirred for 3 h (Figure 7C). As for the carbamate group in the axial *N*-Cbz-glycinate ligand, the intensity of the signal H^i (δ 3.46) was decreased to 40% upon 0.5 h of stirring with D_2O and 10% upon 3 h of stirring (Figure 7). In sharp contrast with the *N*-Cbz-glycinate complex **3d**, the zinc acetate complex **3c** underwent complete deuterium exchange within 0.5 h at both amide moieties of the strap (H^c, δ 3.46; H^h, δ 4.34). Furthermore, as for the unstrapped reference of the zinc *N*-Cbz-glycinate complex **4d** (δ 2.96), the deuterium exchange at the carbamate moiety was again completed within 0.5 h. Thus, in the *N*-Cbz-glycinate complex of the strapped *N*-methylporphyrin **3d**, the strap amide NH on the "non-*N*-Me side" of the receptor and the carbamate NH in the axial ligand participate in hydrogen bond formation.

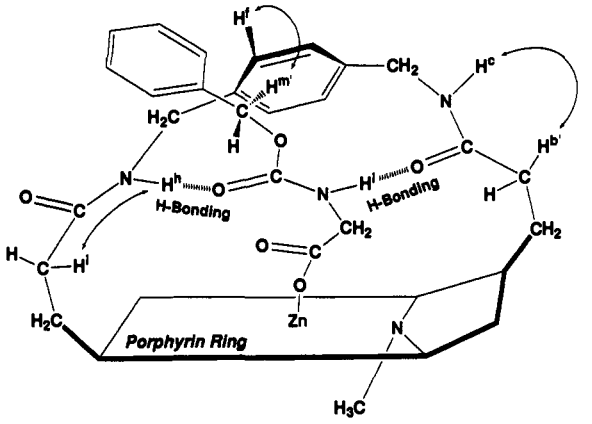

Figure 8. Proposed structure of the zinc *N*-Cbz-glycinate complex of the strapped *N*-methylporphyrin. The arrows indicate the characteristic NOE correlations.

Since NOE observation of **3d** showed connectivities for the pairs $H^c/H^{b'}$ on the "*N*-Me side" and H^h/H^i on the "non-*N*-Me side", the two amide linkages in the receptor take s-trans conformations.[20] Furthermore, as is the case for the zinc acetate complex of the strapped *N*-methylporphyrin **3c**, a NOE cross peak was observed for **3d** between the H^{13} protons and the phenylene protons (H^f), indicating that the fundamental structure of **3d** is identical to that of **3c-B** (Figure 3), where the axial group and the *N*-methyl group are on the same side with respect to the strap. Taking all the above spectroscopic profiles of **3d** into consideration, the structure shown in Figure 8 is most likely, where the carbamate NH and C=O of the substrate are hydrogen bonded respectively to the amide C=O on the "*N*-Me side" and the amide NH on the "non-*N*-Me side" of the receptor. The two-dimensional NOESY spectrum of **3d** showed a cross peak between the benzylic proton $H^{m'}$ in the Cbz group and the phenylene proton H^f in the strap, indicating that the Cbz group in the axial ligand is in proximity to the strap moiety of the receptor. Thus, in the recognition of chiral amino acid anions, the substrate with a NHCO functionality is bound to the receptor via one electrostatic interaction (CO_2^---Zn^+) and two hydrogen bonding interactions (NH--O=C), where attractive and/or repulsive van der Waals forces may additionally operate between the amino acid side chain of the substrate and the strap moiety of the receptor. Consequently, the three-dimensional chiral recognition is accomplished.

The hydrogen bonding interactions in Figure 8 play an important role in the chiral recognition, since enantioselection did not occur at all for *N*-Cbz-*N*-methylalaninate and *N*-Cbz-prolinate having no NHCO functionalities with hydrogen bonding capability (runs 2 and 9, Table 2). In this respect, unlike the *N*-Cbz-glycinate complex **3d**, the N-methylated analogue **3d'** did not show any substantial differences in wavenumbers of both amide C=O (1645 cm^{-1}) and carbamate C=O (1692 cm^{-1}) absorptions from the reference samples; the *acetate* complex of the strapped *N*-methylporphyrin **3c** (amide C=O, 1645 cm^{-1}) and the *N*-Cbz-*N*-methylglycinate complex of the *nonstrapped* porphyrin **4d'** (carbamate C=O, 1695 cm^{-1} (Figure 6 (i, iv, and v)). This observation indicates the absence of any intramolecular hydrogen bonding interaction in **3d'**.

(19) (a) Krauss, E. M.; Chan, S. I. *J. Am. Chem. Soc.* **1982**, *104*, 1824. (b) Krauss, E. M.; Cowburn, D. *Biochemistry* **1981**, *20*, 671. (c) Hawks, G. E.; Randall, E. W.; Hull, W. E.; Gattegno, D.; Conti, F. *Biochemistry* **1978**, *17*, 3986. (d) Thiery, C.; Nabedryk-Viala, E.; Fermandjian, S.; Thiery, J. M. *Biochim. Biophys. Acta* **1977**, *494*, 293.

(20) Boger, D. L.; Yohannes, D.; Zhou, J.; Patane, M. A. *J. Am. Chem. Soc.* **1993**, *115*, 3420.

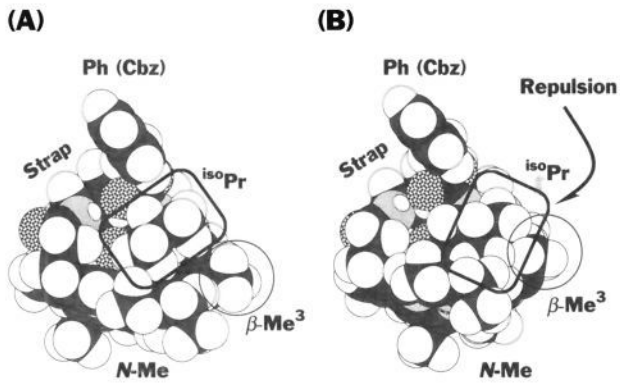

Figure 9. CPK models of favorable (A) and unfavorable (B) diastereoisomers of the zinc strapped *N*-methylporphyrin bound to *N*-Cbz-valinate via two hydrogen bonds and a zinc–carboxylate bond.

In Table 2, valinates (runs 3 and 4), the best substrates for enantioselection, bear larger steric bulks around the asymmetric carbon atoms. On the other hand, alaninate, norvalinate, norleucinate, and leucinate, which are less enantioselectively recognized substrates (runs 1, 6, 7, and 8), have sterically less hindered asymmetric carbon atoms. From these results, we consider that the steric repulsion between the receptor and the steric bulk around the asymmetric center of the substrate is a major determining factor for chiral discrimination. When *N*-Cbz-L-phenylglycinate having an aromatic amino acid side chain is bound to the $[+]_{422}$-receptor, the ^{1}H NMR signal due to H^3 (Figure 2) showed an upfield shift (δ 2.51) from those of the *N*-Cbz-L-valinate (δ 3.23) and *N*-Cbz-L-alaninate (δ 3.26) complexes. Thus, the amino acid side chain in the binding substrate is considered to be located above the N-methylated pyrrole ring. On the basis of this result, CPK models of the favorable and unfavorable diastereoisomers, shown in Figure 9, were constructed for the *N*-Cbz-valinate–$[+]_{422}$-receptor complex **3e** (X = $O_2CC^*H(i\text{-Pr})NHCbz$), where the stereochemistry at the asymmetric nitrogen atom in the receptor adopted is deduced from the CD correlation of **2c** derived from $[+]_{422}$-**3c** with a chiral N-substituted etioporphyrin I family with defined configuration.[17] In the model of the favorable diastereoisomer (Figure 9A), the amino acid side chain (^{iso}Pr) is oriented away from the β-methyl^3 substituent of the receptor so that the steric repulsion between these two parts is minimized. On the contrary, when the configuration of the binding substrate is opposite (unfavorable diastereoisomer (Figure 9B)), the steric repulsion between these two parts is inevitable (circles in Figure 9).

Conclusion

In the present paper, the novel chiral anion-binding receptor **3c**, which enantioselectively recognizes amino acids in the carboxylate form, was presented. The receptor is devoid of any asymmetric carbon atom but is chiral due to the enantiotopic structure of the precursor porphyrin. By taking advantage of the rigid conformation of the metalloporphyrin, the functionalities for electrostatic, hydrogen bonding, and van der Waals interactions are strategically incorporated for achieving three-dimensional molecular recognition. The single extraction experiments of N-protected amino acid sodium salts with **3c** provided an example of the highest level enantioselection of chiral carboxylates reported to date.

Experimental Section

Materials. Tetrahydrofuran (THF) was distilled over sodium benzophenone ketyl just before use. Mesoporphyrin II dimethyl ester (2,12-bis(2′-(methoxycarbonyl)ethyl)-7,17-diethyl-3,8,13,18-tetramethylporphine (**2a**) was synthesized from 4,5-dimethyl-3-(methoxycarbonyl)ethyl)pyrrole-2-carboxylic acid[21] and 3-ethyl-5-formyl-4-methylpyrrole-2-carboxylic acid by a procedure similar to that reported by Collman *et al.*[22] Mesoporphyrin II (**1a**) was obtained by hydrolysis of the dimethyl ester **2a**.[5] *N*-Cbz-*N*-methylglycine and *N*-CBz-DL-*N*-methylalanine were prepared by reaction of carbobenzoxy chloride with *N*-methylglycine (sarcosine) (Tokyo Kasei) and DL-*N*-methylalanine (Sigma), respectively. Other amino acid derivatives were obtained from Tokyo Kasei or Sigma and used as received.

***p*-Xylylene-Strapped Mesoporphyrin II 3a.** To a THF solution (320 mL) of mesoporphyrin II (**1a**) (594 mg, 1.0 mmol) in a 1-L round-bottomed flask equipped with a dropping funnel were successively added triethylamine (0.7 mL, 5.3 mmol) and isobutyl chloroformate (0.31 mL, 2.4 mmol) by means of hypodermic syringes under dry nitrogen at room temperature to convert **1a** into the corresponding mixed anhydride. After the mixture was stirred for 1 h at room temperature, a THF solution (170 mL) of 1,4-xylylenediamine (409 mg, 3.0 mmol) was introduced to the dropping funnel by a syringe and added dropwise to the mixed anhydride solution over a period of 5 h. The mixture was stirred for an additional 36 h at room temperature under dry nitrogen and evaporated to dryness. The residue dissolved in CH_2Cl_2 (200 mL) was filtered from insoluble fractions by passing through Celite, and the filtrate was concentrated to a small volume, which was chromatographed on silica gel (Wakogel C-300). After two red bands were eluted with CH_2Cl_2, a red band was eluted with $CHCl_3$/acetone (90/10 v/v), which was collected and evaporated to dryness, and the residue was recrystallized from CH_2Cl_2/hexane to give **3a** as reddish purple powder (300 mg, 45% yield). FAB-HRMS for $C_{42}H_{46}O_2N_6$ (MH^+): calcd m/z 667.3760; obsd m/z 667.3758. UV–vis ($CHCl_3$) λ_{max}, nm (log ϵ): 620 (3.49), 566 (3.72), 536 (3.86), 501 (3.92), 401 (5.00). ^{1}H NMR: δ 10.15 and 10.05 (s × 2, 4H, meso), 4.74 (ddd, 2H, diastereotopic porph-CH_2CH$_2$CO), 4.21 (m, 6H, diastereotopic porph-CH_2CH$_2$CO (2H) and porph-CH_2CH$_3$ (4H)), 3.74 and 3.57 (s × 2, 12H, porph-CH$_3$), 3.27 (br, 2H, CONH), 2.97 (m, 2H, diastereotopic porph-CH$_2$CH_2CO), 2.62 (d, 4H, CH_2C$_6$H$_4$), 2.49 (s, 4H, C$_6$H$_4$), 2.36 (ddd, 2H, diastereotopic porph-CH$_2$CH_2CO), 1.88 (t, 6H, porph-CH$_2$CH_3), –3.55 (br, 2H, core NH).

***p*-Xylylene-Strapped *N*-Methylporphyrin 3b.** In a 500-mL round-bottomed flask equipped with a reflux condenser were placed **3a** (300 mg, 0.45 mmol), $CHCl_3$ (160 mL), methyl iodide (30 mL, 0.48 mol), and acetic acid (10 mL), and the mixture was stirred at 55 °C. After 40 h, the reaction mixture was poured into saturated aqueous $NaHCO_3$. The isolated organic layer was washed successively with aqueous ammonia (28%) and saturated aqueous NaCl, dried over anhydrous Na_2SO_4, and evaporated to dryness. The residue dissolved in a minimum volume of CH_2Cl_2 was loaded on a silica gel column (Wakogel, C-200) prepared from $CHCl_3$ slurry. Unreacted **3a** was first eluted with $CHCl_3$/acetone (90/10 v/v) as a red band. The red protonated porphyrin fraction remained at the top of the column and was eluted with CH_2Cl_2/ethanol/diethylamine (90/9/1 v/v), collected, and evaporated. Recrystallization of the residue from CH_2Cl_2/hexane gave **3b** as purple powder (153 mg, 50% yield). FAB-HRMS for $C_{43}H_{49}N_6O_2$ (MH^+): calcd m/z 681.3917; obsd m/z 681.3963. UV–vis ($CHCl_3$) λ_{max}, nm (log ϵ): 624 (3.75), 587 (3.78), 535 (3.79), 507 (4.08), 412 (5.00). ^{1}H NMR ($CDCl_3$): δ 10.24, 10.13, 9.98, 9.92 (s × 4, 4H, meso), –4.46 (s, 3H, *N*-CH$_3$). Other signals at δ 0.5–6 ppm were poorly resolved.

Zinc Acetate Complex of *p*-Xylylene-Strapped *N*-Methylporphyrin 3c. To a $CHCl_3$ solution (10 mL) of **3b** (68 mg, 0.1 mmol) was added saturated methanolic Zn(OAc)$_2$ (2 mL), and the mixture was refluxed for 2 h. The reaction mixture was cooled and washed twice with saturated aqueous CH_3CO_2Na. The organic layer was isolated, dried over anhydrous Na_2SO_4, and filtered. The filtrate was evaporated to dryness under reduced pressure, and the residue was recrystallized from CH_2Cl_2/cyclohexane to give **3c** as purple crystals in quantitative yield. Anal. Calcd for $C_{45}H_{50}N_6O_4Zn \cdot CH_2Cl_2 \cdot {}^1/_2C_6H_{12} \cdot H_2O$: C, 61.99; H, 6.37; N, 8.85. Found: C, 62.30; H, 6.26; N, 8.97. The solvates CH_2Cl_2, cyclohexane, and water were quantified by ^{1}H NMR spectroscopy. FAB-MS for $C_{45}H_{50}N_6O_4Zn$ (M^+): calcd m/z 804; obsd m/z 804. FAB-HRMS for $C_{45}H_{47}N_6O_2Zn$ ([M – OAc]$^+$): calcd m/z 743.3052; obsd m/z 743.3052. UV–vis ($CHCl_3$) λ_{max}, nm (log ϵ): 625 (3.40), 583 (3.90), 541 (3.84), 426 (5.04). IR (cm^{-1}): 3291 (br, NH st), 1645 (amide C=O st), 1605 (CO_2^- st), 1523 (amide NH δ).

Zinc *N*-Cbz-Glycinate Complex of *p*-Xylylene-Strapped *N*-Methylporphyrin 3d. To a 20-mL sample bottle containing a $CHCl_3$ solution (5

(21) Chang, C. K. *J. Am. Chem. Soc.* **1977**, *99*, 2819.
(22) Collman, J. P.; Denisevich, P.; Konai, Y.; Marrocco, M.; Koval, C.; Anson, F. C. *J. Am. Chem. Soc.* **1980**, *102*, 6027.

mL) of the zinc acetate complex **3c** (40 mg, 50 μmol) was added *N*-Cbz-glycine (105 mg, 0.5 mmol) dissolved in 0.1 N aqueous NaOH (5 mL), and the mixture was vigorously stirred at room temperature. After 10 h, the organic layer was isolated, washed with water, dried over anhydrous Na_2SO_4, and evaporated to dryness. The residue was recrystallized from CH_2Cl_2/cyclohexane to give **3d** as purple crystals (95% yield). FAB-MS for $C_{53}H_{57}O_6N_7Zn$ (M^+): calcd *m/z* 951; obsd *m/z* 951. FAB-MS for $[M - O_2CCH_2NHCO_2CH_2C_6H_5]^+$: calcd *m/z* 743; obsd *m/z* 743. IR (cm^{-1}): 3600–3200 (br, amide and carbamate, NH st), 1703 (carbamate C=O st), 1645 and 1622 (amide C=O st), 1605 (CO_2^- st), 1535 and 1508 (amide and carbamate NH δ).

Other *N*-Cbz amino acid complexes such as **3e** and **4e** were similarly prepared.

Transformation of 3b into the Zinc Acetate Complex of *N*-Methylmesoporphyrin II Dimethyl Ester (2c). To a 50-mL round-bottomed flask containing **3b** (15 mg, 22 mmol) was added 3 N HCl (4 mL), and the mixture was refluxed. After 3 h, the reaction mixture was poured into saturated aqueous $NaHCO_3$, and the isolated organic layer was washed successively with saturated aqueous NaCl, dried over anhydrous Na_2SO_4, and evaporated to dryness to give *N*-methylmesoporphyrin II (**1b**) in quantitative yield, which was dissolved in MeOH containing one drop of H_2SO_4 to esterify the CO_2H moieties in **1b**. After being stirred in the dark overnight, the mixture was poured into saturated aqueous $NaHCO_3$, and the organic layer was isolated, washed with saturated aqueous NaCl, dried over anhydrous Na_2SO_4, and evaporated to dryness to give *N*-methylmesoporphyrin II dimethyl ester (**2b**). The free base (**2b**) was converted into the zinc acetate complex (**2c**) similarly to the preparation of **3c** (15 mg, 93% yield). FAB-MS for $C_{37}H_{43}N_4O_4Zn$ ($[M - OAc]^+$): calcd *m/z* 671; obsd *m/z* 671. UV–vis ($CHCl_3$) λ_{max}, nm (log ε): 624 (3.75), 587 (3.78), 535 (3.79), 507 (4.08), 412 (5.00). ^1H NMR ($CDCl_3$): δ 9.98, 9.92 (s × 2, 4H, meso), 4.50–4.22 (overlapped m, 4H, porph-CH_2CH_2), 4.15–3.92 (m, 4H, CH_2CH_3), 3.76–3.66 (overlapped, porph-CH_3 × 2 and OCH_3), 3.48 and 3.46 (overlapped, s × 2, 3H × 2, porph-CH_3 and OCH_3), 3.22 (s, porph-CH_3, 3H), 3.28 (apparently t, diastereotopic porph-CH_2CH_2CO), 2.76 (apparently t, diastereotopic porph-CH_2CH_2CO), 1.80 and 1.76 (t × 2, 3H × 2, CH_2CH_3), –4.72 (s, 3H, *N*-CH_3).

Direct N-Methylation of Mesoporphyrin II Dimethyl Ester (2a). A regioisomeric mixture of the zinc acetate complex of *N*-methylmesoporphyrin II dimethyl ester (**2c-A,B**) was obtained in 58% yield by reaction of methyl iodide with **2a** and subsequent metalation with $Zn(OAc)_2$ as described for the preparation of **3b,c**. The ^1H NMR spectrum in $CDCl_3$ showed a broad signal at δ –1.04 due to the axial acetate groups and two singlet signals at δ –4.64 and –4.78 due to the *N*-methyl groups.

Optical Resolutions by HPLC. Resolution of the optical antipodes of **3c** was carried out by using a 4.6- × 250-mm (analytical) or 20- × 500-mm (preparative) HPLC column packed with silica gel coated with cellulose tris(3,5-dimethylphenylcarbamate) as a chiral stationary phase (Daicel Chiralcel OD). HPLC experiments with the analytical column were performed on a JASCO Type TWINCLE equipped with a JASCO Type 875-UV variable wavelength detector at a flow rate of 1.0 mL·min^{-1} at room temperature and monitored at 390 nm. HPLC experiments with the preparative column were performed on a JASCO Type 887-PU pump equipped with a JASCO Type 875-UV variable wavelength detector, a JASCO Type 802-SC system controller, and a JASCO Type 892-01 column selector at a flow rate of 10.0 mL·min^{-1} at room temperature and monitored at 550 nm.

For milligram-scale resolution, 3-mL portions of a 2-propanol solution of **3c** (200 mg in 20 mL) were loaded repeatedly on the preparative column with hexane/2-propanol/acetic acid (70/30/1 v/v) as the eluent. Since the peak resolution was poor, the eluate was divided into three fractions, and the optical isomers ($[+]_{422}$-**3c** and $([-]_{422}$-**3c**) were obtained from the first and last fractions, respectively. The second fraction was again subjected to the HPLC resolution. The fractionated isomers were converted into the free bases and purified by column chromatography on alumina ($CHCl_3$) followed by metalation with $Zn(OAc)_2$ to give the antipodes of **3c**. $[+]_{422}$-**3c**: recovery 74%, 100% ee (from HPLC analysis on an analytical column). $[-]_{422}$-**3c**: recovery 35%, 97% ee.

Single-Extraction Experiments. A $CHCl_3$ (2 mL) solution of **3c** (10 μmol) was stirred for 10 h with an aqueous solution (2 mL) of the substrate (100 μmol) at room temperature. The organic layer was isolated, washed with water, dried over Na_2SO_4, and filtered, and the residue after stripping off the volatile fraction was subjected to ^1H NMR analysis in $CDCl_3$ (0.5 mL). **3c** was quantitatively converted into **3e** in every case. The diastereoisomer ratio of **3e** was determined on the basis of the relative intensity of the two well-separated *N*-methyl signals, since the signals due to the axial ligand were poorly separated except for the cases of the alaninate and valinate complexes.

Measurements. ^1H and ^{13}C NMR spectra were measured in $CDCl_3$ on a JEOL Type GSX-270 spectrometer operating at 270 and 67.5 MHz, respectively, at 25 °C unless otherwise noted. Chemical shift values (ppm) were determined with respect to internal $CHCl_3$ (^1H, δ 7.28; ^{13}C, δ 77.10). ^1H–^1H double-quantum-filtered (DQF) COSY spectra were recorded with eight scans and 256 t_1 increments using the pulse sequence D_1–90°–t_1–90°–D_2–90°–acquisition with a 90° pulse of 8.0 μs and relaxation delays D_1 = 2 s and D_2 = 10 μs. ^1H–^1H NOESY spectra were recorded with 32 scans and 256 t_1 increments using the pulse sequence D_1–90°–t_1–90°–τ_{mix}–90°–acquisition with a 90° pulse of 8.0 μs, relaxation delay D_1 = 2 s, and mixing time τ_{mix} = 300, 500, or 700 ms. In each 2D NMR, the spectral width in both dimensions was 5000 Hz, and after zero filling, the final size of the data matrix was 512 × 1024. Apodization with a squared sine bell function was used in both dimensions.

Absoption spectra were measured in $CHCl_3$ on a JASCO Type U-best 50 spectrometer at 25 °C by using a quartz cell of 1-cm path length. Infrared spectra were measured in $CHCl_3$ on a JASCO Type IR-5300 spectrometer at 25 °C using a NaCl cell. Circular dichroism spectra were recorded at 25 °C on a Jasco Type J-720 spectropolarimeter with the following parameters: sensitivity, 10 mdeg; step resolution, 2 nm/data; response, 4 s; scan speed, 50 nm·min^{-1}; accumulation, 16 times, using a quartz cell of 1-cm path length; optical density of sample ($CHCl_3$), 2.0 at 424 nm. FAB-MS measurements were performed on a JEOL JMS-HX110 spectrometer using a 3-nitrobenzyl alcohol matrix.

Acknowledgment. The present work was partly supported by Grant-in-Aid No. 04225206 for Scientific Research on a Priority Area from the Ministry of Education, Science, and Culture, Japan. We also thank Dr. Naoko Morisaki of the Institute of Molecular and Cellular Biosciences, University of Tokyo, for FAB-MS measurements.